Developmental Cell *10*, 625–634, May, 2006 ©2006 Elsevier Inc. DOI 10.1016/j.devcel.2006.03.009

Heparan Sulfate in *trans* Potentiates VEGFR-Mediated Angiogenesis

Lars Jakobsson,[1] Johan Kreuger,[1] Katarina Holmborn,[2] Lars Lundin,[1] Inger Eriksson,[2] Lena Kjellén,[2] and Lena Claesson-Welsh[1,3,*]
[1] Department of Genetics and Pathology
Uppsala University
Rudbeck Laboratory
Dag Hammarskjöldsv. 20
SE-75185 Uppsala
Sweden
[2] Department of Medical Biochemistry and Microbiology
Uppsala University
Biomedical Center
Box 582
SE-75123 Uppsala
Sweden

Summary

Several receptor tyrosine kinases require heparan sulfate proteoglycans (HSPGs) as coreceptors for efficient signal transduction. We have studied the role of HSPGs in the development of blood capillary structures from embryonic stem cells, a process strictly dependent on signaling via vascular endothelial growth factor receptor-2 (VEGFR-2). We show, by using chimeric cultures of embryonic stem cells defective in either HS production or VEGFR-2 synthesis, that VEGF signaling in endothelial cells is fully supported by HS expressed in *trans* by adjacent perivascular smooth muscle cells. Transactivation of VEGFR-2 leads to prolonged and enhanced signal transduction due to HS-dependent trapping of the active VEGFR-2 signaling complex. Our data imply that direct signaling via HSPG core proteins is dispensable for a functional VEGF response in endothelial cells. We propose that transactivation of tyrosine kinase receptors by HSPGs constitutes a mechanism for crosstalk between adjacent cells.

Introduction

Heparan sulfate proteoglycans (HSPGs) are transmembrane, glycosylphosphatidylinositol-anchored or secreted proteins with covalently linked heparan sulfate (HS) chains that modulate the activity of a large number of secreted signaling molecules. HS is a linear, N- and O-sulfated glycosaminoglycan expressing diverse sulfated epitopes that constitute binding sites for protein ligands. More than 100 proteins have been reported to interact with the HS moiety of HSPGs, or with heparin, a related but more highly sulfated polysaccharide produced and released only by connective tissue-type mast cells (Bernfield et al., 1999; Esko and Selleck, 2002). HSPGs are present in high copy numbers on cell surfaces, and expressed by most cells in mammalian tissues (Bernfield et al., 1999). HSPGs have been implicated in many aspects of growth factor function, such as in formation of higher order receptor complexes (Yayon et al., 1991) and in growth factor transport and gradient formation (Belenkaya et al., 2004; Han et al., 2005; Kirkpatrick et al., 2004; Kreuger et al., 2004; The et al., 1999). Several angiogenic growth factors, such as vascular endothelial growth factor (VEGF)-A, fibroblast growth factor (FGF)-2, and platelet-derived growth factor (PDGF)-BB, depend on HS/heparin for full biological effect (Gitay-Goren et al., 1992; Rolny et al., 2002; Yayon et al., 1991). Heparin can partially compensate for the lack of HS expression in several tissue culture models, presumably by serving as a scaffold that facilitates or stabilizes the interaction between growth factors and their receptors. Physiologically, however, heparin and HS appear to have distinct and nonoverlapping functions.

Binding of growth factors to HS/heparin is regulated by differential sulfation of the polysaccharide backbone, creating a multitude of protein binding domains (Kreuger et al., 2005). The bifunctional enzymes of the N-deacetylase/N-sulfotransferase (NDST) family catalyze early steps in HS biosynthesis that are crucial for proper HS sulfation (Grobe et al., 2002). There are four vertebrate NDST isoforms, of which NDST1 and 2 display broad and overlapping tissue distribution. Gene inactivation of murine NDST1 leads to a dramatic reduction in N- and O-sulfation of HS in most basement membranes. The majority of NDST1-deficient embryos survive until birth but die shortly thereafter in a condition resembling respiratory distress syndrome (Fan et al., 2000; Ringvall et al., 2000). Elimination of NDST2 expression is compatible with survival and fertility, but the mice are unable to synthesize sulfated heparin (Forsberg et al., 1999). Combined inactivation of the *Ndst1* and *2* genes results in early embryonic lethality (K.H. and L.K., unpublished data). HS produced by *Ndst1/2*$^{-/-}$cells is devoid of both N-sulfate and 2-O-sulfate groups, while a low level of 6-O-sulfation remains (Holmborn et al., 2004).

During vascular development, blood vessels are formed through in situ differentiation of mesodermal precursor cells denoted angioblasts into endothelial cells (Flamme et al., 1997). Maturation of the vasculature involves pruning of vessels and eventually formation of capillaries from preexisting vessels, a process known as angiogenesis. Stabilization of the newly formed vessel requires production of a specialized basement membrane and attraction of supporting perivascular smooth muscle cells, pericytes. Inactivation of the gene for VEGF-A or one of its receptors, VEGFR-2 (alternatively denoted Flk-1/KDR to indicate murine or human species, respectively), severely impairs vasculogenesis and hematopoiesis in the embryo, leading to embryonic death (Ferrara et al., 1996; Shalaby et al., 1995). VEGF-A/VEGFR-2 are critical also in physiological vessel maintenance in the adult (Kamba et al., 2006). Furthermore, most, if not all, tumors produce VEGF-A, leading to excessive and deregulated pathological angiogenesis.

*Correspondence: lena.welsh@genpat.uu.se
[3] Lab address: http://www.genpat.uu.se/Welsh_Vascular_Biology

The VEGF-A gene encompasses nine alternatively spliced exons (for a review, see Olsson et al., 2006) that give rise to protein isoforms with different biological properties. The shortest isoform, VEGF-A121, lacks the HS binding domain and is freely diffusible. The most commonly expressed isoform, VEGF-A165, includes the HS binding domain and is retained at the cell surface or in the extracellular matrix (Leung et al., 1989; Park et al., 1993; Tischer et al., 1989).

We show here through coculture of stem cells defective in either HSPG or VEGFR-2 production that HSPGs expressed in *trans* relative to VEGFRs support formation of functional VEGFR complexes with enhanced signaling properties in response to VEGF-A165 but not VEGF-A121. This represents a mechanism for HS-dependent transactivation regulating signaling and turnover of tyrosine kinase receptors.

Results and Discussion

The objective of this study was to define the role of HS in VEGFR-2 signaling and the subsequent development of endothelial cells and capillary structures. As a model, we used clusters of differentiating mouse embryonic stem (ES) cells, designated embryoid bodies, which faithfully mimic early steps of vascular development (Magnusson et al., 2004; Vittet et al., 1996). Wild-type embryoid bodies responded to VEGF-A165 with formation of a peripheral vascular plexus consisting of sprouting capillary-like structures (Figure 1A). In contrast, embryonic stem cells established from *Ndst1/2*$^{-/-}$ blastocysts failed to respond to VEGF-A165 (Figure 1A). The lack of response of the *Ndst1/2*$^{-/-}$ embryoid bodies is in agreement with the fact that NDST enzymes catalyze early steps in the sulfation of HS/heparin, and that VEGF-A165 is a heparin binding growth factor (Ruhrberg et al., 2002). Inclusion of heparin or purified HS in the embryoid body cultures over a wide range of concentrations and for different time periods in the presence of VEGF-A165 (Figure 1A, and data not shown) consistently failed to support vascular development in the *Ndst1/2*$^{-/-}$ embryoid bodies. Because purified and endogenous HS might differ significantly in degree and pattern of sulfation, we investigated the potential contribution of endogenously produced, soluble HS in VEGFR-2 signaling. This was accomplished through transwell coculture of HS-producing *vegfr-2*$^{-/-}$ embryoid bodies with *Ndst1/2*$^{-/-}$ embryoid bodies placed in tissue culture inserts (see Figure 1B for experimental setup). The *vegfr-2*$^{-/-}$ cells secreted readily detectable levels of HS that diffused into the upper chamber (Figure 1C, and data not shown). Despite the presence of soluble wild-type HS in the culture medium, inclusion of VEGF-A165 failed to induce vessel formation in the *Ndst1/2*$^{-/-}$ embryoid bodies, compared with control wild-type embryoid bodies that responded to VEGF-A165 with formation of a richly branched endothelial cell plexus (Figure 1D). Moreover, conditioned medium from *vegfr-2*$^{-/-}$ cultures was transferred onto *Ndst1/2*$^{-/-}$ embryoid bodies, which also failed to support vascular development (data not shown). Taken together, these results show that attenuation of NDST1/2 expression interrupts VEGF-A165-dependent vascular development, and this process is not rescued by soluble HS/heparin.

A well-established nitrocellulose filter binding assay (Kreuger et al., 2003) was employed to investigate the binding of HS/heparin to VEGF. Figure 1E shows that VEGF-A165, but not VEGF-A121, bound heparin although not to the same extent as an equimolar concentration of the positive control, FGF-2. Moreover, HS purified from *vegfr-2*$^{-/-}$ stem cells, but not from *Ndst1/2*$^{-/-}$ stem cells, efficiently bound VEGF-A165 (Figure 1F).

To test whether the *Ndst1/2*$^{-/-}$ embryoid bodies could be rescued by cell-associated HS, we designed a chimeric stem cell culture model where *Ndst1/2*$^{-/-}$ stem cells were mixed at different ratios with *vegfr-2*$^{-/-}$ stem cells and thereafter allowed to differentiate in response to VEGF-A165. Importantly, embryoid bodies derived exclusively from either *Ndst1/2*$^{-/-}$ or *vegfr-2*$^{-/-}$ stem cells failed to undergo vascular development (Figures 1A and 2). In contrast, a striking rescue with endothelial cell differentiation and vascular plexus formation was seen in VEGF-A165-treated embryoid bodies composed of a mixture of *Ndst1/2*$^{-/-}$ and *vegfr-2*$^{-/-}$ stem cells at ratios of 1:9, 1:1, and 9:1 (*Ndst1/2*$^{-/-}$:*vegfr-2*$^{-/-}$; see Figure 2).

Alteration in HS production or sulfation can be expected to have global effects on growth factor signaling. Consequently, the recorded lack of vascular development by *Ndst1/2*$^{-/-}$ embryoid bodies could be due to a partial or complete arrest in mesoderm formation. We therefore analyzed transcript levels of genes expressed within the mesoderm (*vegfr-2*, *pdgfr-*β, and *brachyury*) and the endoderm (*afp* and *gata-4*) by PCR from reverse transcripts prepared from wild-type, *Ndst1/2*$^{-/-}$, *vegfr-2*$^{-/-}$, or chimeric 9:1 (*Ndst1/2*$^{-/-}$:*vegfr-2*$^{-/-}$; hereafter denoted chimeras) embryoid bodies, at different stages of differentiation. Transcripts of *vegfr-2* and *pdgfr-*β were detected at day 4 and 8 in embryoid bodies derived from *Ndst1/2*$^{-/-}$, wild-type, and chimeric cultures and the transcripts persisted in the wild-type and chimeric bodies until day 12. As expected, there were no *vegfr-2* transcripts expressed in the *vegfr-2*$^{-/-}$ stem cells (see Table 1; based on Figure S1A in the Supplemental Data available with this article online). *brachyury* transcripts were absent in the *Ndst1/2*$^{-/-}$ cultures under the conditions used here, whereas the kinetics of expression of *brachyury* in the chimeras followed that of wild-type, only at lower levels. The expression of the endoderm-derived α-fetoprotein (*afp*) was comparable in chimeras and wild-type but delayed in *Ndst1/2*$^{-/-}$ cultures. *gata-4* mRNA was undetectable in *Ndst1/2*$^{-/-}$ stem cells as well as in the chimeras. These results indicate defects in mesodermal and endodermal differentiation in *Ndst1/2*$^{-/-}$ stem cells and partial genotypic rescue in the chimeric embryoid bodies, allowing for a complete rescue of vascular development (Figure 2).

To analyze the potential genotypic drift over time in the chimeric embryoid bodies, we studied expression of *Ndst2* by real-time PCR (Figure S1B). Because *Ndst2* was absent in the *Ndst1/2*$^{-/-}$ cells, this analysis reflects an estimate of the *vegfr-2*$^{-/-}$ pool within the chimeras. Although 90% of the cells lacked *Ndst2* at day 0, the expression at day 4, 8, and 12 was 62%, 63%, and 77% of that in *vegfr-2*$^{-/-}$, respectively, indicating a genetic drift toward the *vegfr-2*$^{-/-}$ genotype. In chimeras treated with VEGF, however, staining revealed an increased pool of VEGFR-2-positive cells, illustrating an

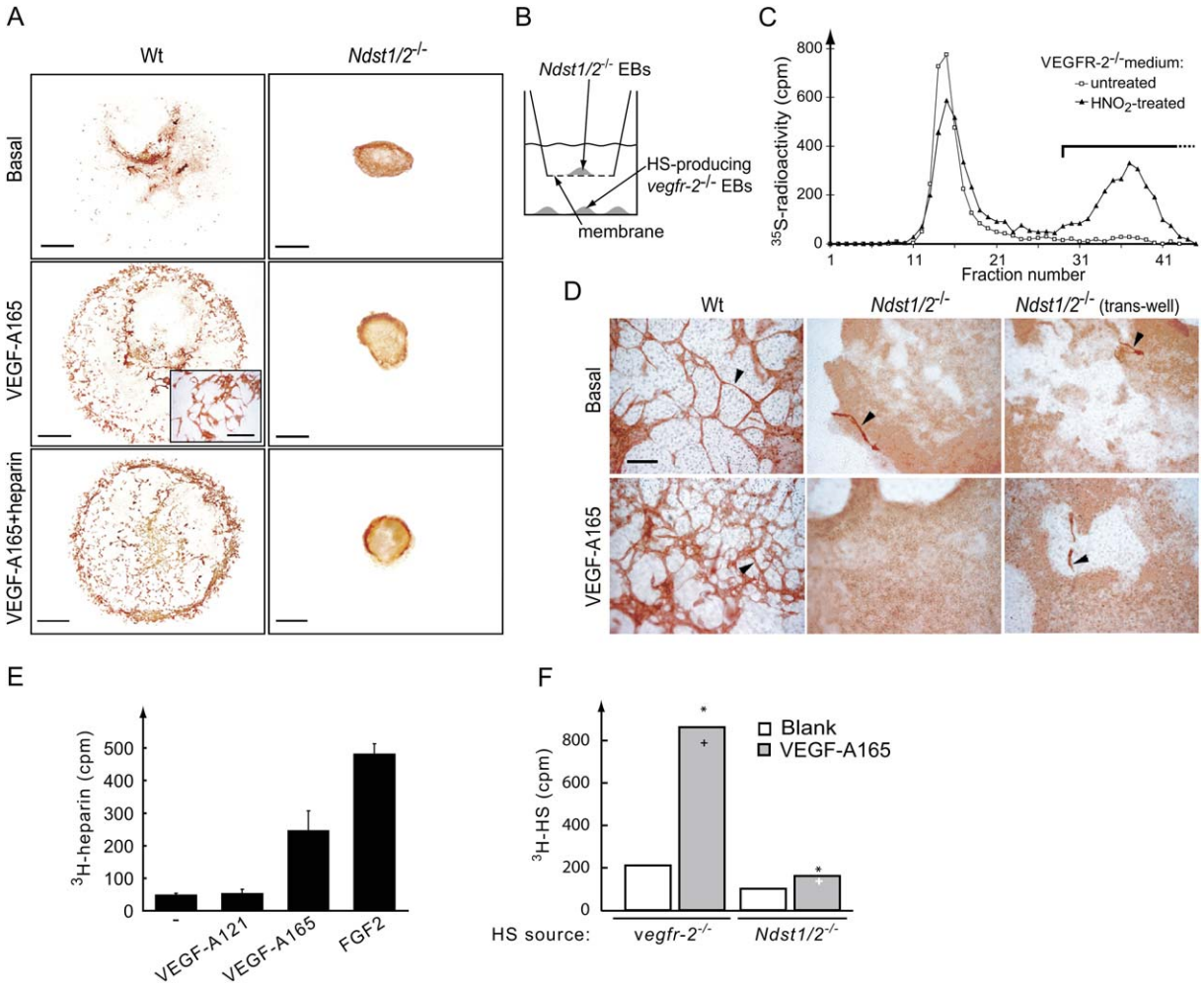

Figure 1. Both Soluble HS and Heparin Fail to Rescue Endothelial Cell Development in *Ndst1/2*$^{-/-}$ Embryoid Bodies

(A) Wild-type (Wt) but not *Ndst1/2*$^{-/-}$ embryoid bodies develop vascular structures. Embryoid bodies formed from wild-type or *Ndst1/2*$^{-/-}$ embryonic stem cells were seeded on glass slides in the absence (basal) or presence of VEGF-A165 (30 ng/ml) and heparin (100 ng/ml). At day 10, the bodies were fixed and stained for expression of CD31. The scale bar represents 1 mm. Inset shows higher magnification of the vascular plexus. The scale bar represents 100 μm.

(B) Experimental setup for transwell experiments.

(C) Embryoid bodies secrete HS into the medium. Eight-day-old embryoid bodies were metabolically labeled with [^{35}S]sulfate overnight. Radiolabeled glycosaminoglycans (GAGs) were isolated from the medium and separated on Sephadex G50 before (open box) or after (triangles) HNO_2 digestion to degrade HS. The distribution of radioactivity before and after digestion shows that 46% of total GAGs retrieved from the medium were HS.

(D) Soluble HS does not rescue vascular development in *Ndst1/2*$^{-/-}$ ES cells. *Ndst1/2*$^{-/-}$ ES cells were differentiated in conditioned medium from *vegfr-2*$^{-/-}$ cultures until day 4 and further cultured in tissue culture inserts with *vegfr-2*$^{-/-}$ embryoid bodies, secreting HS, in the bottom of the well. The bodies were stained for expression of CD31 after 6 days of differentiation in the transwell setup. Arrowheads indicate capillary structures. The scale bar represents 100 μm.

(E) VEGF-A165 and FGF-2, but not VEGF-A121, bind to heparin. The bars indicate standard deviation.

(F) VEGF-A165 binds HS isolated from *vegfr-2*$^{-/-}$ embryoid bodies, but not HS purified from *Ndst1/2*$^{-/-}$ embryoid bodies. The graph illustrates the mean of two measuring points (* and + indicate highest and lowest value, respectively).

expansion of *Ndst1/2*$^{-/-}$-derived endothelial cells (Figure 3). These data demonstrate the plasticity of the model employed, allowing expansion of different subpopulations of cell lineages depending on the context.

A model of invasive angiogenesis was employed to identify VEGFR-2- and HS-expressing cell types contributing to the development of vascular structures in the chimeric embryoid bodies. For this purpose, embryoid bodies were cultured in three-dimensional collagen I gels and stimulated with VEGF-A165 to induce outgrowth of capillary-like structures into the surrounding matrix. Neither *Ndst1/2*$^{-/-}$ nor *vegfr-2*$^{-/-}$ embryoid bodies responded to VEGF-A165 (Figure 3A), whereas wild-type as well as chimeric cultures responded vigorously by extending sprouts of endothelial cells (CD31- and VEGFR-2-double positive; Figures 3B and 3C) covered with perivascular smooth muscle cells (verified as α smooth muscle actin [αSMA]-positive; Figure 3D), hereafter denoted pericytes. We conclude that the *Ndst1/2*$^{-/-}$ stem cells serve as the source for VEGFR-2-expressing endothelial cells in the chimeric cultures.

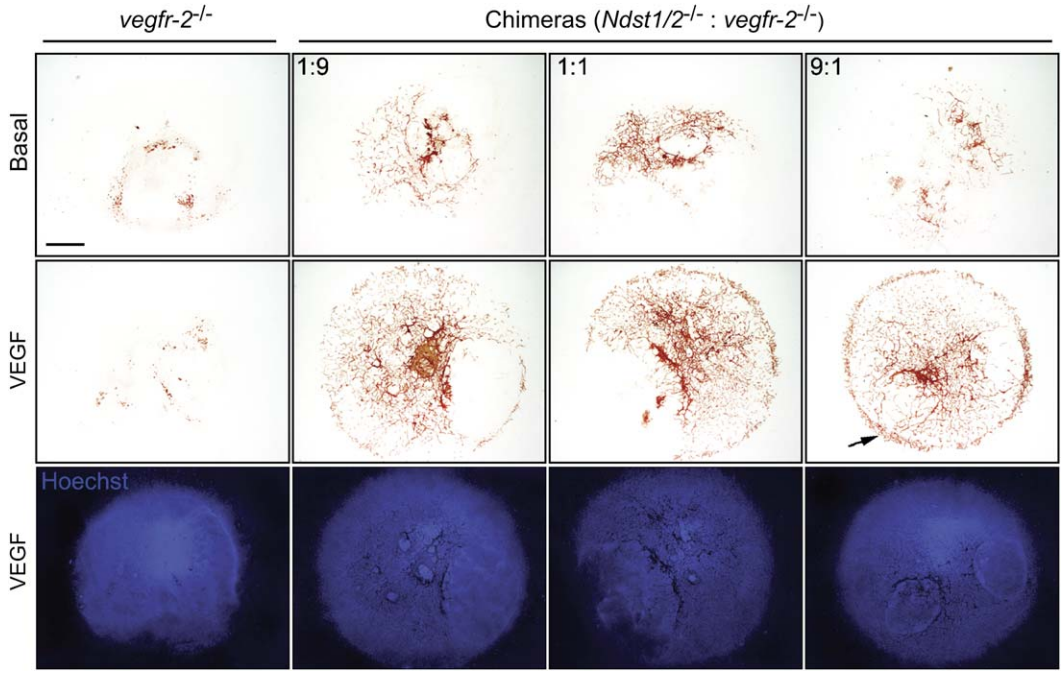

Figure 2. Chimeras of *vegfr-2*$^{-/-}$ and *Ndst1/2*$^{-/-}$ ES Cells Allow Rescue of Vascular Development in Response to VEGF-A165

Ndst1/2$^{-/-}$ and *vegfr-2*$^{-/-}$ embryonic stem cells were mixed at different ratios (*Ndst1/2*$^{-/-}$: *vegfr-2*$^{-/-}$ at 1:9, 1:1, or 9:1 ratios as indicated) to create chimeric embryoid bodies, which were cultured in the presence or absence of VEGF-A165. The bodies were stained for expression of CD31 on day 10 (shown in red). In parallel, bodies were stained with Hoechst to visualize nuclei (lower panel). Arrow indicates CD31-positive capillary plexus. The scale bar represents 1 mm.

Cells expressing wild-type HS were identified with a monoclonal antibody, HepSS-1, which recognizes highly sulfated epitopes in wild-type HS. HepSS-1 showed reactivity for both endothelial cells and pericytes in angiogenic sprouts in the wild-type embryoid bodies (Figure 4A, left panel). However, in the chimeric cultures, HepSS-1 reactivity was restricted to the pericytes (Figure 4A, right panel). Hence, sulfated and functional HS in the VEGF-A165-induced sprouts was expressed only by pericytes derived from *vegfr-2*$^{-/-}$ stem cells (see Figure S2 for costaining for VEGFR-2, αSMA, and HS). This finding suggests that functional VEGFR-2 activation is supported by HSPGs in *trans*.

The critical role of HS for the ability of the chimeric embryoid bodies to respond to VEGF-A165 in the sprouting assay was further demonstrated by enzymatic digestion of HS with heparinase I–III. This treatment resulted in a marked decrease in the number of angiogenic sprouts (Figures 4B and 4C). In accordance with this, exposure of chimeric cultures to VEGF-A121, which lacks the HS binding domain (see Figure 1E), failed to induce angiogenic sprouting (Figures 4D and 4E). Taken together, these data demonstrate an essential role of HS in VEGF-A165/VEGFR-2 complex formation and signaling.

Chimeric embryoid bodies created by mixing *Ndst1/2*$^{-/-}$ and *vegfr-2*$^{-/-}$ ES cells at a 9:1 ratio (i.e., only

Table 1. mRNA Levels of Germ Layer Marker Genes Measured by PCR on Reverse Transcripts Prepared from the Different Embryoid Body Cultures at Day 4, 8, and 12 of Development

Mesodermal Transcripts[a]					Endodermal Transcripts[a]	
Days of Culture	Genotype	*vegfr-2*	*pdgfr-β*	*brachyury*	*afp*	*Gata-4*
4	*Ndst1/2*$^{-/-}$	+ + +	+ +	—	—	—
	Wt	+ + + +	+ + + +	+ + + +	+ +	+ + +
	9:1	+ +	+	+ +	+ +	—
	vegfr-2$^{-/-}$	—	+ +	+ + +	+	+ + + +
8	*Ndst1/2*$^{-/-}$	+ + +	+ + +	—	—	—
	Wt	+ + + +	+ + + +	+ + +	+ + + +	+ + +
	9:1	+ + +	+ + +	+	+ + + +	—
	vegfr-2$^{-/-}$	—	+ + +	+ +	+ + + +	+ + + +
12	*Ndst1/2*$^{-/-}$	—	+ + +	—	+	—
	Wt	+ + +	+ + + +	+ +	+ + + +	+ + +
	9:1	+ + +	+ + + +	—	+ + + +	—
	vegfr-2$^{-/-}$	—	+ + + +	+ +	+ + + +	+ + + +

[a] Transcript levels are indicated as absent (−) or from low (+) to high (+ + + +) as estimated from PCR band intensities (see Figure S1A).

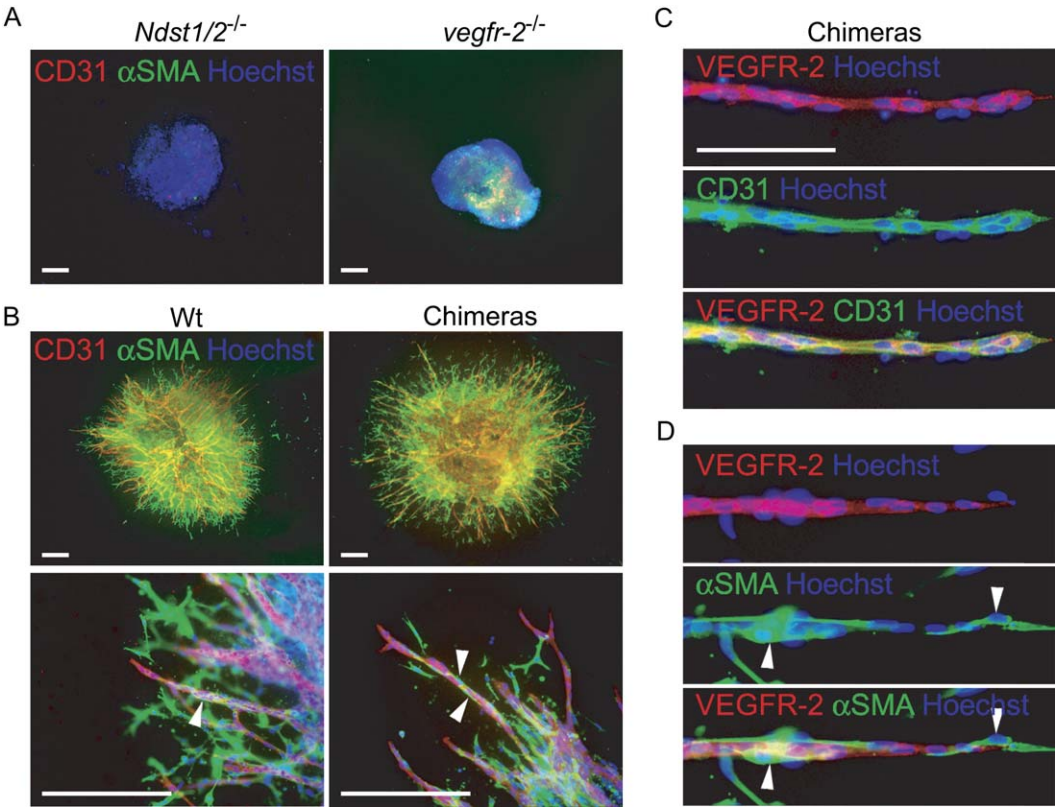

Figure 3. Chimeric Embryoid Bodies Produce Normal Sprouts in 3D Collagen Gels

(A and B) *Ndst1/2*$^{-/-}$, *vegfr-2*$^{-/-}$, chimeric, and wild-type (Wt) embryoid bodies were placed in 3D collagen gels at day 4 and cultured with VEGF-A165 until day 10. The embryoid bodies were stained (whole-mount) for expression of CD31 (red) and αSMA (green).

(A) The VEGFR-2- and NDST1/2-deficient embryoid bodies failed to respond to VEGF-A165.

(B) In contrast, both wild-type and chimeric embryoid bodies displayed a halo of CD31-positive sprouts, surrounded by αSMA-positive cells, which invaded the collagen gel (arrowheads). The scale bars represent 300 μm.

(C) Endothelial cells in the chimeras coexpressed CD31 and VEGFR-2, hence they were derived from the *Ndst1/2*$^{-/-}$ cells expressing VEGFR-2. The scale bar represents 100 μm.

(D) Surrounding cells were negative for these markers but positive for αSMA (arrowheads).

10% HS-producing *vegfr-2*$^{-/-}$ ES cells; see Figure 2) still responded vigorously to VEGF-A165 treatment. This motivated a closer examination of the properties of VEGFR-2 activation and turnover in the chimeric embryoid bodies. As shown in Table 1, *vegfr-2* transcripts were detected in differentiating embryoid bodies derived from *Ndst1/2*$^{-/-}$, chimeric, and wild-type cultures, but not in *vegfr-2*$^{-/-}$ embryoid bodies. In agreement, immunoblotting showed two bands (see Figure S3A), corresponding in size to the described VEGFR-2 forms differing in extent of N-linked glycosylation (Takahashi and Shibuya, 1997), that were expressed at lower levels in the *Ndst1/2*$^{-/-}$ and the chimeric cultures than in the wild-type. It is noteworthy that the lower expression level of VEGFR-2 in the chimeras compared to wild-type embryoid bodies did not reflect a reduced number of endothelial cells, as suggested by both immunostaining (Figure 3B) and immunoblotting (see Figure 5D) for the endothelial cell marker CD31. The slightly reduced mobility of VEGFR-2 in the chimeric cultures was at least in part due to changes in glycosylation, as judged from digestion with N-glycosidase F (data not shown). Treatment of the wild-type embryoid bodies with VEGF-A165 induced activation of VEGFR-2 as indicated by tyrosine phosphorylation of the receptor (Figure 5A), but with slower kinetics than that previously noticed in serum-starved endothelial cell monolayer cultures (Singh et al., 2005). Studies in such models have shown that receptor tyrosine kinases become rapidly internalized in response to ligand binding; concomitantly, there is an increased rate of protein synthesis and transport of newly synthesized receptors to the cell surface (Eriksson et al., 1991; Kremer et al., 1997). The chimeric cultures also responded to VEGF-A165 with tyrosine phosphorylation of the receptor. Remarkably, VEGFR-2 protein levels and receptor tyrosine phosphorylation persisted in the chimeras and increased over the first 2 hr (Figure 5A; see quantification in Figure 5B). In contrast, the expression of VEGFR-2 protein in the wild-type embryoid bodies decreased after 1–3 hr of stimulation, followed by a restoration to basal levels (see Figure S3B). Analysis over longer time periods showed that phosphorylated VEGFR-2 (in relation to VEGFR-2 protein) increased in the chimeras followed by a gradual decrease to the basal level by 24 hr (Figure 5C). In the wild-type embryoid bodies, a much smaller fraction of receptors became tyrosine phosphorylated in relation to the total VEGFR-2 pool. Consistently, we observed at

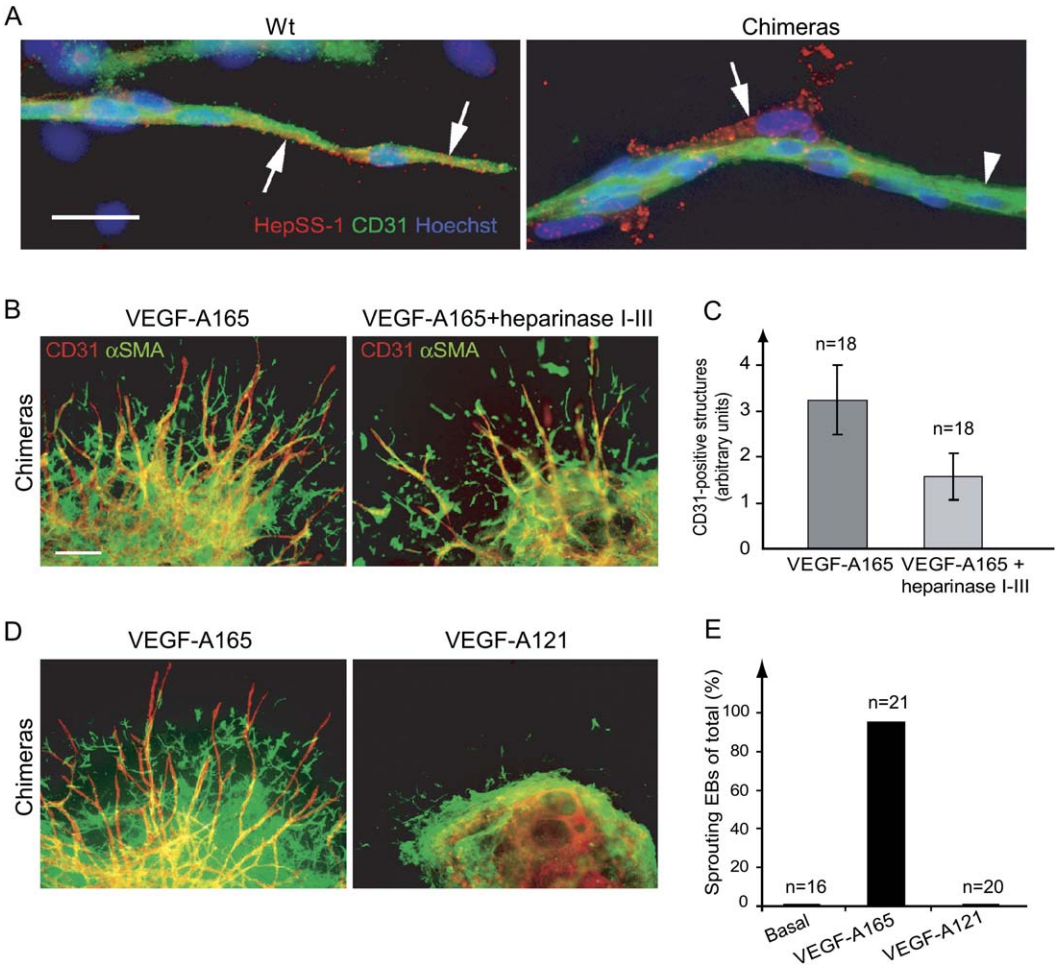

Figure 4. Pericytes Present HS in *trans* to Endothelial Cells in Angiogenic Sprouts in the Chimeras

(A) Embryoid bodies from wild-type (Wt; left) stem cells or from chimeric (right) cultures were seeded in 3D collagen gels in the presence of VEGF-A165. Immunofluorescent staining showed colocalization of CD31 (green) and HS (red; visualized by staining with the HepSS-1 antibody) on endothelial cells in the wild-type embryoid bodies (arrows in the wild-type panel). In the chimeric cultures, HS was localized on pericytes (arrow) adjacent to the CD31-positive endothelial cells (arrowhead), in agreement with the fact that wild-type HS was produced only by cells derived from *vegfr-2*$^{-/-}$ ES cells. Hoechst staining (blue) was performed to visualize nuclei. The scale bar represents 50 μm. For VEGFR-2, HS, and αSMA costaining, see Figure S2.

(B) Digestion of HS by heparinase I–III reduced the VEGF-induced response. The scale bar represents 200 μm.

(C) Quantification of CD31-positive structures in chimeric embryoid bodies (in Figure 4B) with or without HS digestion. The bars indicate standard deviation.

(D) The nonheparin binding VEGF isoform 121 did not induce endothelial cell sprouting.

(E) Quantification of the fraction of embryoid bodies positive for sprouting in (D).

least a 10-fold higher fraction of activated receptors in the chimeras compared to wild-type. VEGFR-2 expressed in the *Ndst1/2*$^{-/-}$ embryoid bodies failed to respond to VEGF-A165 (data not shown) due to the HS deficiency, and were not further analyzed with regard to signaling or turnover.

In a pulse-chase analysis, cultures were exposed to VEGF-A165 for a limited period of time, followed by washing and continued culture in complete medium (Figure 5D). Thereby, the induction and clearance of a limited pool of tyrosine-phosphorylated VEGFR-2 could be followed over time, without continuous inclusion of newly activated receptors as in Figures 5A–5C (where cultures were exposed to growth factor throughout the experiment). As seen in Figure 5E, the level of phospho-VEGFR-2 increased dramatically (about 20-fold) in the chimeric embryoid bodies, and remained for several hours. In contrast, the wild-type cultures displayed a 2-fold, transient increase in phosphorylated VEGFR-2. The moderate amplitude in VEGFR-2 phosphorylation in the wild-type compared to chimeras might in part be a consequence of the higher basal phosphorylation in the wild-type setting (Figure 5D). Moreover, in the wild-type, HS may interact with the receptor complex both in *cis* and in *trans*, which complicates a direct comparison with the "in *trans* only" chimeric condition. However, we conclude that VEGF-A165-induced signaling is potentiated by HSPGs presented in *trans* to the receptor and that HS-dependent trapping of VEGFR-2 results in an accumulation of receptors, instead of downregulation as in the wild-type situation, with prolonged activation as a consequence.

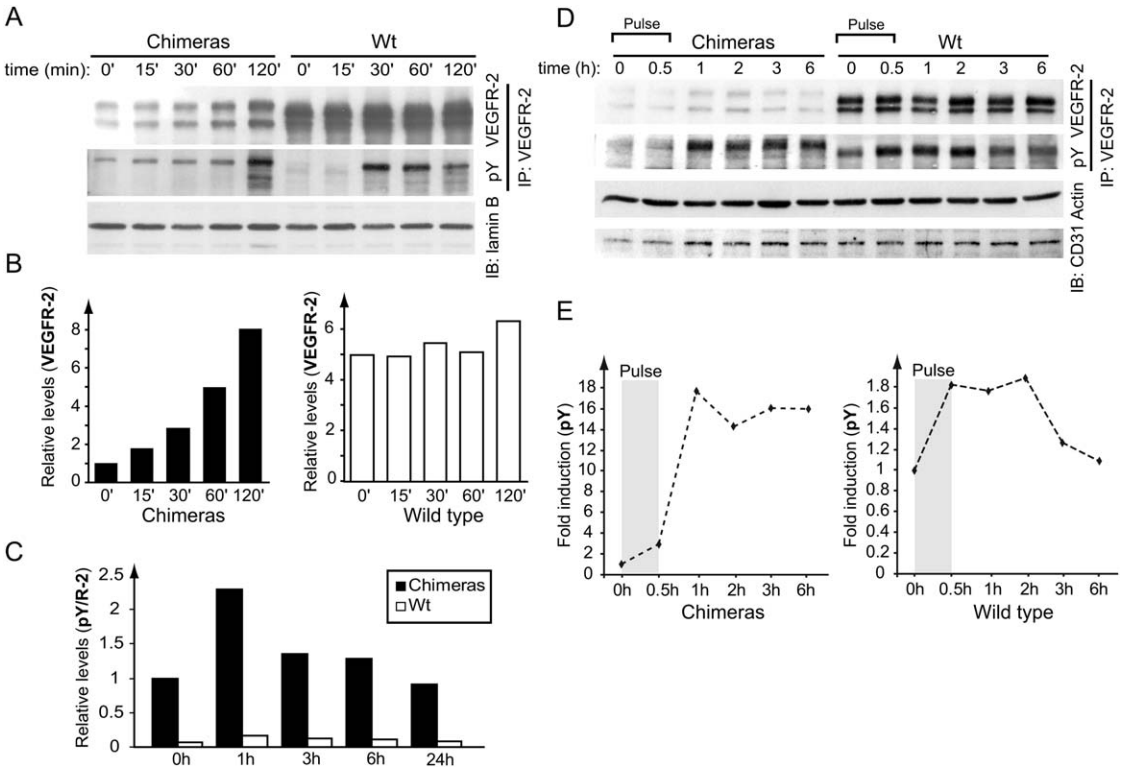

Figure 5. HS in *trans* Potentiates VEGFR-2 Activation and Signaling

(A) Chimeric and wild-type embryoid bodies (day 11) were exposed to VEGF-A165 and harvested at different time points. VEGFR-2 protein was immunoprecipitated (IP), followed by immunoblotting (IB) for phosphotyrosine (pY), for VEGFR-2, or as a control for equal loading, for laminB. The slightly reduced mobility of VEGFR-2 in the chimeric cultures is at least in part due to changes in glycosylation, as judged from digestion with N-glycosidase F (data not shown).

(B) Quantification of VEGFR-2 expression in (A) shows that levels increased over time in the chimeras.

(C) Quantification of tyrosine-phosphorylated VEGFRs relative to total VEGFR-2 protein following VEGF-A165 stimulation for 0, 1, 3, 6, and 24 hr (the immunoblot used for quantification is shown in Figure S3B).

(D) Clearance of VEGFR-2 in embryoid bodies pulsed with VEGF-A165 for 30 min followed by washing and "chase" in full growth medium. Cultures harvested at different time points were analyzed by IP/IB for phospho-VEGFR-2 and total VEGFR-2 protein. Equal loading was controlled by blotting for actin. Blotting for CD31, a vascular marker, shows similar expression levels in different cultures.

(E) Quantification of phosphorylated receptors in (D) illustrating differential signaling kinetics in wild-type and chimeric embryoid bodies.

We suggest that transactivation of VEGFR-2 by HSPGs presented by pericytes or perivascular cell types, alternatively by the extracellular matrix/basement membrane, efficiently captures receptor complexes at the cell surface. Thereby, internalization and degradation of phosphorylated receptors is delayed, allowing efficient utilization of activated receptors in transduction of biological responses (Figure 6).

The sulfation of HS is subject to strict developmental control in a tissue- and age-dependent manner (Feyzi et al., 1998). Our data support the notion that the sulfation of HSPGs is crucial for the regulation of cell differentiation in a physiological setting. We show that VEGF-A165 readily interacts with wild-type HS, but not with undersulfated HS derived from *Ndst1/2*$^{-/-}$ stem cells, and that sprouting angiogenesis is sensitive to HS degradation. VEGF-A121, which is unable to bind heparin/HS, failed to induce angiogenic sprouting (cf. Figure 4D). In agreement with our data, path finding of vascular sprouts in the developing retina is impaired in mice expressing only the VEGF-A120 isoform (corresponding to the human VEGF-A121), pointing to a role for HSPGs in guidance of vascular sprouts by modulating VEGF gradient formation (Ruhrberg et al., 2002). It is conceivable that part of the rescue of blood endothelial cell differentiation seen here in chimeric cultures is due to a restored VEGF-A165 gradient formation. Interestingly, not only VEGF-A165, but also VEGFR-2, displays an HS/heparin binding motif (Dougher et al., 1997). In addition, coreceptors for VEGFs of the neuropilin family interact with HS/heparin (Mamluk et al., 2002). Thus, all components in the putative VEGF-A165/VEGFR-2/neuropilin signaling complex have the capacity to bind directly to HS. Our data suggest that the stability and turnover of VEGFR-2 is modulated by HSPGs. The delay in clearance of VEGFR-2 that we observed in the chimeric cultures is reminiscent of data on reduced FGFR internalization in the presence of N-cadherin, leading to increased FGFR stability and enhanced biological responses (Suyama et al., 2002). The half-life of the active signaling complex may be regulated not only by the rate of internalization but also by decreasing the off-rate of the ligand as described for FGF/heparin/FGFR complexes (Ibrahimi et al., 2004). The prolonged half-life may in turn lead to an enhanced or altered pattern of tyrosine phosphorylation. In accordance, we have previously shown that inclusion of heparin is a prerequisite for FGF-2-induced phosphorylation of the C-terminal

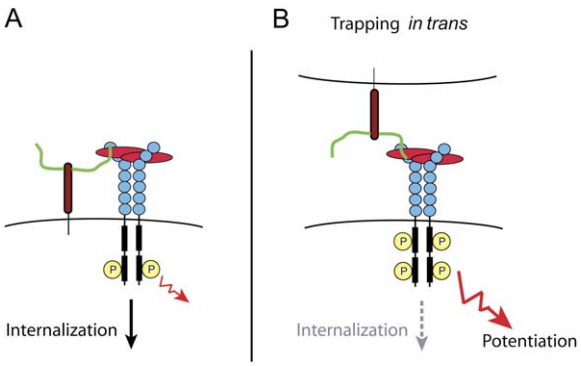

Figure 6. Model for Transactivation of VEGFR-2 by HS

(A) In the wild-type situation, the VEGFR-2 (blue) and VEGF (light red) complex is bound to HS (green line) provided by the endothelial cell itself.

(B) In the chimeras, where the VEGFR-2-positive endothelial cells lack functional HS, the receptor-ligand complex is stabilized by HS provided in *trans*, leading to trapping of the signaling VEGFR complex at the cell surface and delayed internalization and degradation of activated VEGFRs. Stabilization of the active signaling complex may preserve and even enhance receptor phosphorylation (indicated by P).

tail tyrosine residue 766 in FGFR-1, whereas the juxtamembrane domain tyrosine residue 463 is phosphorylated both in the absence and presence of heparin (Lundin et al., 2003). In vivo, differential expression of HSPGs as well as temporal and spatial regulation of distinct protein binding HS epitopes may play a major role in regulating signaling, not only by ligand binding, but also as shown here, by modulating receptor turnover.

As a consequence of the experimental setup, we can infer that direct signaling of the HS-bearing core protein is dispensable for endothelial cell development, as only properly sulfated and thus functional HSPG core proteins exist in *trans* on pericytes, and not in endothelial cells. Pericytes serve an important role in stabilization and maturation of the vasculature; dissociation of pericytes leads to endothelial cell apoptosis and vessel regression. The molecular mechanisms in the close interplay between pericytes and endothelial cells resulting in vessel survival are still poorly understood (Armulik et al., 2005). It is possible that pericyte/endothelial cell transcommunication involving efficient HS-dependent presentation of growth factors such as VEGF-A165 is critical in vessel stability.

It is noteworthy that the NDST1/2 deficiency most likely hampered general development by affecting multiple HS-dependent processes, in addition to VEGF-dependent ones. This is indicated by the delayed and apparently defective endoderm development in the *Ndst1/2*$^{-/-}$ ES cells (Table 1). Whether endoderm-derived inductive signals are required for proper vasculogenesis such as in formation of vascular tubes is disputed (Jin et al., 2005; Pardanaud et al., 1996; Vokes and Krieg, 2002). The rescue of the *Ndst1/2*$^{-/-}$ phenotype by *vegfr-2*$^{-/-}$ ES cells may therefore have been exerted on more than one level, by supplying normal endoderm to facilitate general development and by supplying cell surface HS to allow signal transduction through the VEGF/VEGFR-2 complex.

In conclusion, we propose a mechanism whereby HSPGs in *trans* may regulate VEGFR-2 signaling. This finding has two major implications: first, it demonstrates an intrinsic robustness of the VEGFR signaling pathway, such that local, cell-autonomous deficiencies in HS production can be fully rescued by adjacent cells. We note that several studies have shown that adjacent cell populations differ significantly with regard to expression of HS epitopes, providing an in vivo context for such transactivation (Dennissen et al., 2002). Second, our findings demonstrate that transactivation via HSPGs may be an additional avenue for crosstalk between adjacent cells. The general consequences of such crosstalk for other HSPG-dependent tyrosine kinase receptors, such as the FGF and PDGF receptors, require further investigation.

Experimental Procedures

Embryonic Stem Cells

Murine 129 SvJ, R1 wild-type and *vegfr-2*$^{-/-}$ embryonic stem cells (Shalaby et al., 1995) were kind gifts of Dr. Andras Nagy and Dr. Janet Rossant, Samuel Lunenfeld Research Institute, Mount Sinai Hospital, Toronto, Canada, respectively. The *Ndst1/2*$^{-/-}$ ES cells were established as described by Holmborn et al. (2004).

Embryoid Bodies

ES cell clones were cultured in Dulbecco's modified Eagle's medium/glutamax (Invitrogen), 25 mM HEPES, 1.2 mM sodium pyruvate, 19 mM monothioglycerol (Sigma), 15% fetal bovine serum, and 1000 units/ml leukemia inhibitory factor (LIF). At day 0, 1200 cells were aggregated in hanging drops (20 μl) without LIF, in the presence or absence of 0.79 nM human recombinant VEGF-A165 (PeproTech) or VEGF-A121 (R&D), with or without 1, 10, or 100 ng/ml heparin (Inolex Pharmaceutical Division) or 1, 10, 100, or 1000 ng/ml HS from pig intestinal mucosa (a gift from G. van Dedem, Diosynth, The Netherlands). Chimeric cultures of *Ndst1/2*$^{-/-}$ and *vegfr-2*$^{-/-}$ ES cells were established at 1:9, 1:1, or 9:1 ratios. At day 4, the embryoid bodies were placed in 8-well glass culture slides (BD Falcon) or in a collagen I suspension composed of Ham's F12 medium (Promocell), 6.26 mM NaOH, 20 mM HEPES, 0.117% $NaHCO_3$, 1% glutamax I (GIBCO), and 1.5 mg/ml collagen I (Cohesion). Medium with or without growth factors was changed at day 8.

Immunostaining of Embryoid Bodies

At day 10, embryoid bodies on glass slides were processed for whole-mount immunohistochemical staining as described previously (Magnusson et al., 2004). Embryoid bodies in collagen gels were fixed in 4% p-formaldehyde in phosphate-buffered saline (PBS), blocked, and permeabilized in 3% bovine serum albumin (BSA), 0.2% Triton X-100 in PBS, followed by sequential overnight incubations with primary and secondary antibodies. Hoechst 33342 was used to visualize the nuclei. The samples were analyzed in either a Nikon Eclipse E1000 microscope with a Nikon Eclipse DXM 1200 camera (Nikon) or an LSM 510 META confocal microscope (Carl Zeiss). The following primary antibodies were used: rat anti-mouse CD31 antibody (PharMingen), fluorescein isothiocyanate-conjugated mouse monoclonal anti-α smooth muscle actin antibody, goat anti-mouse VEGFR-2 (R&D), rabbit anti-VEGFR-2 (Cell Signaling), and IgM mouse anti-mouse HepSS-1 antibody (Seikagaku). Secondary antibodies were: Alexa 568 goat anti-rat IgG, Alexa 488 goat anti-rat IgG, Alexa 555 donkey anti-goat IgG or Alexa 555 goat anti-mouse IgM (Molecular Probes), Cy5 donkey anti-rabbit IgG (Jackson ImmunoResearch), biotinylated goat anti-rat IgG antibody, and horseradish peroxidase-conjugated streptavidin (Vector).

Transwell Cultures

From day 0 to day 4, *Ndst1/2*$^{-/-}$ ES cells were allowed to differentiate in hanging drops with conditioned medium from wild-type embryoid bodies. At day 4, the bodies were put individually in 24-well

cell culture inserts with 1 μm pore size membranes (BD Falcon). To condition the medium in the insert cultures, *vegfr-2*$^{-/-}$ embryoid bodies were seeded in the bottom of the wells 2 days prior to seeding of *Ndst1/2*$^{-/-}$ bodies in the inserts. The *Ndst1/2*$^{-/-}$ bodies in the inserts were cultured for 6 days after seeding. For experimental setup, see Figure 1B.

Characterization of ^{35}S-Labeled Glycosaminoglycans

Embryoid bodies cultured for 8 days were metabolically labeled for 22 hr with 330 μCi of [^{35}S]sulfate in 5.5 ml of culture medium. After incubation, ^{35}S-labeled glycosaminoglycans were isolated from the medium as previously described (Holmborn et al., 2004). After treatment with 0.5 M NaOH for 18 hr at 4ºC followed by neutralization, the labeled glycosaminoglycans were analyzed by gel chromatography on Sephadex G50 superfine (0.5 × 100 cm) before and after deamination with HNO_2 at pH 1.5. This treatment results in cleavage of HS at N-sulfated GlcN residues but leaves chondroitin sulfate intact. The column was eluted in 0.2 M NH_4HCO_3 and fractions of 0.5 ml were collected and analyzed for ^{35}S radioactivity.

Binding Assay

^{3}H-labeled HS was isolated from *Ndst1/2*$^{-/-}$ and *vegfr-2*$^{-/-}$ embryoid bodies after metabolic labeling with [^{3}H]glucosamine (33 μCi/ml) for 24 hr as previously described (Holmborn et al., 2004). ^{3}H-heparin was a kind gift from Dr. Dorothe Spillmann, Uppsala University, Sweden. The binding of radiolabeled heparin/HS to VEGF-A121 and -165 and FGF-2 was analyzed with the nitrocellulose (NC) filter binding assay, as described by Kreuger et al. (2003). Briefly, the different growth factors were incubated with radiolabeled saccharide (7,000 cpm of [^{3}H]heparin with 26 nmol growth factor, or 10,000 cpm of [^{3}H]HS with 130 nmol growth factor) in 50 μl PBS at room temperature for 15 min. The mixture was then rapidly passed through an NC filter, where proteins and protein-bound saccharides bind to the filter whereas free saccharides pass through. NC filters together with protein-bound [^{3}H]HS or [^{3}H]heparin were analyzed for radioactivity by scintillation counting.

Heparinase Digestion

Embryoid bodies were cultured in collagen with VEGF-A165 (30 ng/ml). At day 6, a mixture of heparinase-I, -II, and -III (IBEX Pharmaceuticals) was added to the cultures at a final concentration of 3.4 mU/ml for each enzyme. This addition was repeated after 18 hr and 24 hr. At day 8, fresh medium was supplied with addition of another 3.4 mU/ml heparinase I–III followed by one final addition of fresh enzymes 24 hr later. Embryoid bodies were fixed at day 10 and stained for CD31, as described above. Total area of positive structures in a total of 18 embryoid bodies per condition was quantified with image analysis. Error bars represent standard deviation of the mean.

Reverse Transcription Polymerase Chain Reaction

Total RNA was prepared from wild-type, *Ndst1/2*$^{-/-}$, chimeric, and *vegfr-2*$^{-/-}$ embryoid bodies cultured in tissue culture dishes for 4, 8, and 12 days, by using an RNeasy mini kit (Qiagen). Samples were DNase I treated (Qiagen) and RNA levels were determined by spectrophotometry. One microgram of RNA from each condition was used for reverse transcription (Upstate Biochemicals) to create cDNA. The condition for the cDNA synthesis was 37ºC for 1 hr and 95ºC for 5 min. Primers were designed by using PrimerExpress 1.5a (Applied Biosystems) and synthesized by Invitrogen. The PCR conditions were 95ºC for 10 min, (95ºC, 15 s/60ºC, 60 s) × 35 cycles. The primer pairs used were: 5′-CACTATTGGCAACGAGCGG-3′, 5′-GACAGAGGCGATGAATGGTG-3′ for *vegfr-2*, 5′-GTGGTGAACTTCCAATGGACG-3′, 5′-GTCTGTCACTGGCTCCACCAG-3′ for *pdgfr-β*, 5′-TAAGGAACCACCGGTCATCG-3′, 5′-TTGTCCGCATAGGTTGGAGAG-3′ for *brachyury*, 5′-ACCCCTTCATGTATGCCCC-3′, 5′-GCATGCCAGAACGACCTTG-3′ for *α-fetoprotein*, 5′-AGCTCCATGTCCCAGACTTCA-3′, 5′-AGCAGACAGCACTGGATGGAT-3′ for *Gata-4*, and 5′-CACTATTGGCAACGAGCGG-3′, 5′-TCCATACCCAAGAAGGAAGGC-3′ for *β-actin*. In the analysis of *Ndst2* mRNA levels, primers were: 5′-TGGACCGGTACTGTGTGGAG-3′, 5′-GGGCTCGGAAAAAGCCA-3′. Real-time PCR with SYBR Green PCR master mix was run and detected in an ABI Prism 7700 instrument (Applied Biosystems). The expression levels were normalized to *β*-actin.

Immunoblotting

Embryoid bodies were seeded in complete medium in tissue culture dishes at day 4. At day 11, the cultures were stimulated for 0, 15, 30, 60, 90, or 120 min with VEGF-A165 at 100 ng/ml in complete medium. For the pulse-chase analysis, embryoid bodies were pulsed with VEGF-A165 for 30 min at 37ºC followed by extensive washes and thereafter "chased" in full growth medium. The cells were lysed in 20 mM Tris HCl (pH 7.5), 150 mM NaCl, 10% glycerol, 1% NP40, 2 mM EDTA, 500 μM Na_3VO_4, 1% aprotinin, 10 μg/ml leupeptin, and 1 mM phenylmethyl sulfonylfluoride. The protein concentration was measured with the BCA protein detection kit (Pierce) and adjusted for equal loading. For immunoprecipitation, lysates were incubated with goat anti-mouse VEGFR-2 (R&D) for 1.5 hr at 4ºC followed by incubation with fast-flow protein-G-Sepharose (Amersham Biosciences), end over end, at 4ºC for 45 min. Proteins were released by boiling in sample buffer (59 mM Tris-HCl [pH 6.8], 1.5% SDS, 4.35% glycerol, 4% β-mercaptoethanol, 0.0025% bromophenol blue) and separated with SDS-PAGE. The following primary antibodies were used: mouse anti-phospho-tyrosine (4G10; Cell Signaling), goat anti-mouse laminB, goat anti-mouse CD31, and goat anti-actin (Santa Cruz Biotechnology). Immunoreactivity was visualized by enhanced chemiluminescence. Quantification of immunoreactive bands was made in Image Gauge (Fujifilm).

Supplemental Data

Supplemental Data include three figures and are available at http://www.developmentalcell.com/cgi/content/full/10/5/625/DC1/.

Acknowledgments

This study was supported by grants to L.C.-W. from the Swedish Cancer Society (project 3820-B04-09XAC), Swedish Research Council (project K2005-32X-12552-08A), and the Novo Nordisk Foundation, and to L.K. from the Swedish Research Council, Gustaf V:s 80-årsfond and Polysackaridforskning AB. J.K. is supported by the Wenner-Gren Foundations.

Received: May 25, 2005
Revised: February 3, 2006
Accepted: March 20, 2006
Published: May 8, 2006

References

Armulik, A., Abramsson, A., and Betsholtz, C. (2005). Endothelial/pericyte interactions. Circ. Res. *97*, 512–523.

Belenkaya, T.Y., Han, C., Yan, D., Opoka, R.J., Khodoun, M., Liu, H., and Lin, X. (2004). *Drosophila* Dpp morphogen movement is independent of dynamin-mediated endocytosis but regulated by the glypican members of heparan sulfate proteoglycans. Cell *119*, 231–244.

Bernfield, M., Gotte, M., Park, P.W., Reizes, O., Fitzgerald, M.L., Lincecum, J., and Zako, M. (1999). Functions of cell surface heparan sulfate proteoglycans. Annu. Rev. Biochem. *68*, 729–777.

Dennissen, M.A., Jenniskens, G.J., Pieffers, M., Versteeg, E.M., Petitou, M., Veerkamp, J.H., and van Kuppevelt, T.H. (2002). Large, tissue-regulated domain diversity of heparan sulfates demonstrated by phage display antibodies. J. Biol. Chem. *277*, 10982–10986.

Dougher, A.M., Wasserstrom, H., Torley, L., Shridaran, L., Westdock, P., Hileman, R.E., Fromm, J.R., Anderberg, R., Lyman, S., Linhardt, R.J., et al. (1997). Identification of a heparin binding peptide on the extracellular domain of the KDR VEGF receptor. Growth Factors *14*, 257–268.

Eriksson, A., Nister, M., Leveen, P., Westermark, B., Heldin, C.H., and Claesson-Welsh, L. (1991). Induction of platelet-derived growth factor α- and β-receptor mRNA and protein by platelet-derived growth factor BB. J. Biol. Chem. *266*, 21138–21144.

Esko, J.D., and Selleck, S.B. (2002). Order out of chaos: assembly of ligand binding sites in heparan sulfate. Annu. Rev. Biochem. *71*, 435–471.

Fan, G., Xiao, L., Cheng, L., Wang, X., Sun, B., and Hu, G. (2000). Targeted disruption of NDST-1 gene leads to pulmonary hypoplasia and neonatal respiratory distress in mice. FEBS Lett. *467*, 7–11.

Ferrara, N., Carver-Moore, K., Chen, H., Dowd, M., Lu, L., O'Shea, K.S., Powell-Braxton, L., Hillan, K.J., and Moore, M.W. (1996). Heterozygous embryonic lethality induced by targeted inactivation of the VEGF gene. Nature *380*, 439–442.

Feyzi, E., Saldeen, T., Larsson, E., Lindahl, U., and Salmivirta, M. (1998). Age-dependent modulation of heparan sulfate structure and function. J. Biol. Chem. *273*, 13395–13398.

Flamme, I., Frolich, T., and Risau, W. (1997). Molecular mechanisms of vasculogenesis and embryonic angiogenesis. J. Cell. Physiol. *173*, 206–210.

Forsberg, E., Pejler, G., Ringvall, M., Lunderius, C., Tomasini-Johansson, B., Kusche-Gullberg, M., Eriksson, I., Ledin, J., Hellman, L., and Kjellen, L. (1999). Abnormal mast cells in mice deficient in a heparin-synthesizing enzyme. Nature *400*, 773–776.

Gitay-Goren, H., Soker, S., Vlodavsky, I., and Neufeld, G. (1992). The binding of vascular endothelial growth factor to its receptors is dependent on cell surface-associated heparin-like molecules. J. Biol. Chem. *267*, 6093–6098.

Grobe, K., Ledin, J., Ringvall, M., Holmborn, K., Forsberg, E., Esko, J.D., and Kjellen, L. (2002). Heparan sulfate and development: differential roles of the N-acetylglucosamine N-deacetylase/N-sulfotransferase isozymes. Biochim. Biophys. Acta *1573*, 209–215.

Han, C., Yan, D., Belenkaya, T.Y., and Lin, X. (2005). *Drosophila* glypicans Dally and Dally-like shape the extracellular Wingless morphogen gradient in the wing disc. Development *132*, 667–679.

Holmborn, K., Ledin, J., Smeds, E., Eriksson, I., Kusche-Gullberg, M., and Kjellen, L. (2004). Heparan sulfate synthesized by mouse embryonic stem cells deficient in NDST1 and NDST2 is 6-O-sulfated but contains no N-sulfate groups. J. Biol. Chem. *279*, 42355–42358.

Ibrahimi, O.A., Zhang, F., Hrstka, S.C., Mohammadi, M., and Linhardt, R.J. (2004). Kinetic model for FGF, FGFR, and proteoglycan signal transduction complex assembly. Biochemistry *43*, 4724–4730.

Jin, S.W., Beis, D., Mitchell, T., Chen, J.N., and Stainier, D.Y. (2005). Cellular and molecular analyses of vascular tube and lumen formation in zebrafish. Development *132*, 5199–5209.

Kamba, T., Tam, B.Y., Hashizume, H., Haskell, A., Sennino, B., Mancuso, M.R., Norberg, S.M., O'Brien, S.M., Davis, R.B., Gowen, L.C., et al. (2006). VEGF-dependent plasticity of fenestrated capillaries in the normal adult microvasculature. Am. J. Physiol. Heart Circ. Physiol. *290*, H560–H576.

Kirkpatrick, C.A., Dimitroff, B.D., Rawson, J.M., and Selleck, S.B. (2004). Spatial regulation of Wingless morphogen distribution and signaling by Dally-like protein. Dev. Cell *7*, 513–523.

Kremer, C., Breier, G., Risau, W., and Plate, K.H. (1997). Up-regulation of flk-1/vascular endothelial growth factor receptor 2 by its ligand in a cerebral slice culture system. Cancer Res. *57*, 3852–3859.

Kreuger, J., Lindahl, U., and Jemth, P. (2003). Nitrocellulose filter binding to assess binding of glycosaminoglycans to proteins. Methods Enzymol. *363*, 327–339.

Kreuger, J., Perez, L., Giraldez, A.J., and Cohen, S.M. (2004). Opposing activities of Dally-like glypican at high and low levels of Wingless morphogen activity. Dev. Cell *7*, 503–512.

Kreuger, J., Jemth, P., Sanders-Lindberg, E., Eliahu, L., Ron, D., Basilico, C., Salmivirta, M., and Lindahl, U. (2005). Fibroblast growth factors share binding sites in heparan sulfate. Biochem J. *389*, 145–150.

Leung, D.W., Cachianes, G., Kuang, W.J., Goeddel, D.V., and Ferrara, N. (1989). Vascular endothelial growth factor is a secreted angiogenic mitogen. Science *246*, 1306–1309.

Lundin, L., Ronnstrand, L., Cross, M., Hellberg, C., Lindahl, U., and Claesson-Welsh, L. (2003). Differential tyrosine phosphorylation of fibroblast growth factor (FGF) receptor-1 and receptor proximal signal transduction in response to FGF-2 and heparin. Exp. Cell Res. *287*, 190–198.

Magnusson, P., Rolny, C., Jakobsson, L., Wikner, C., Wu, Y., Hicklin, D.J., and Claesson-Welsh, L. (2004). Deregulation of Flk-1/vascular endothelial growth factor receptor-2 in fibroblast growth factor receptor-1-deficient vascular stem cell development. J. Cell Sci. *117*, 1513–1523.

Mamluk, R., Gechtman, Z., Kutcher, M.E., Gasiunas, N., Gallagher, J., and Klagsbrun, M. (2002). Neuropilin-1 binds vascular endothelial growth factor *165*, placenta growth factor-2, and heparin via its b1b2 domain. J. Biol. Chem. *277*, 24818–24825.

Olsson, A.K., Dimberg, A., Kreuger, J., and Claesson-Welsh, L. (2006). VEGF receptor signalling–in control of vascular function. Nat. Rev. Mol. Cell Biol. *7*, in press.

Pardanaud, L., Luton, D., Prigent, M., Bourcheix, L.M., Catala, M., and Dieterlen-Lievre, F. (1996). Two distinct endothelial lineages in ontogeny, one of them related to hemopoiesis. Development *122*, 1363–1371.

Park, J.E., Keller, G.A., and Ferrara, N. (1993). The vascular endothelial growth factor (VEGF) isoforms: differential deposition into the subepithelial extracellular matrix and bioactivity of extracellular matrix-bound VEGF. Mol. Biol. Cell *4*, 1317–1326.

Ringvall, M., Ledin, J., Holmborn, K., van Kuppevelt, T., Ellin, F., Eriksson, I., Olofsson, A.M., Kjellen, L., and Forsberg, E. (2000). Defective heparan sulfate biosynthesis and neonatal lethality in mice lacking N-deacetylase/N-sulfotransferase-1. J. Biol. Chem. *275*, 25926–25930.

Rolny, C., Spillmann, D., Lindahl, U., and Claesson-Welsh, L. (2002). Heparin amplifies platelet-derived growth factor (PDGF)-BB-induced PDGF α-receptor but not PDGF β-receptor tyrosine phosphorylation in heparan sulfate-deficient cells. Effects on signal transduction and biological responses. J. Biol. Chem. *277*, 19315–19321.

Ruhrberg, C., Gerhardt, H., Golding, M., Watson, R., Ioannidou, S., Fujisawa, H., Betsholtz, C., and Shima, D.T. (2002). Spatially restricted patterning cues provided by heparin-binding VEGF-A control blood vessel branching morphogenesis. Genes Dev. *16*, 2684–2698.

Shalaby, F., Rossant, J., Yamaguchi, T.P., Gertsenstein, M., Wu, X.F., Breitman, M.L., and Schuh, A.C. (1995). Failure of blood-island formation and vasculogenesis in Flk-1-deficient mice. Nature *376*, 62–66.

Singh, A.J., Meyer, R.D., Band, H., and Rahimi, N. (2005). The carboxyl terminus of VEGFR-2 is required for PKC-mediated down-regulation. Mol. Biol. Cell *16*, 2106–2118.

Suyama, K., Shapiro, I., Guttman, M., and Hazan, R.B. (2002). A signaling pathway leading to metastasis is controlled by N-cadherin and the FGF receptor. Cancer Cell *2*, 301–314.

Takahashi, T., and Shibuya, M. (1997). The 230 kDa mature form of KDR/Flk-1 (VEGF receptor-2) activates the PLC-γ pathway and partially induces mitotic signals in NIH3T3 fibroblasts. Oncogene *14*, 2079–2089.

The, I., Bellaiche, Y., and Perrimon, N. (1999). Hedgehog movement is regulated through tout velu-dependent synthesis of a heparan sulfate proteoglycan. Mol. Cell *4*, 633–639.

Tischer, E., Gospodarowicz, D., Mitchell, R., Silva, M., Schilling, J., Lau, K., Crisp, T., Fiddes, J.C., and Abraham, J.A. (1989). Vascular endothelial growth factor: a new member of the platelet-derived growth factor gene family. Biochem. Biophys. Res. Commun. *165*, 1198–1206.

Vittet, D., Prandini, M.H., Berthier, R., Schweitzer, A., Martin-Sisteron, H., Uzan, G., and Dejana, E. (1996). Embryonic stem cells differentiate in vitro to endothelial cells through successive maturation steps. Blood *88*, 3424–3431.

Vokes, S.A., and Krieg, P.A. (2002). Endoderm is required for vascular endothelial tube formation, but not for angioblast specification. Development *129*, 775–785.

Yayon, A., Klagsbrun, M., Esko, J.D., Leder, P., and Ornitz, D.M. (1991). Cell surface, heparin-like molecules are required for binding of basic fibroblast growth factor to its high affinity receptor. Cell *64*, 841–848.